CrossMark

Coupling antibody based recognition with DNA based signal amplification using an electrochemical probe modified with MnO$_2$ nanosheets and gold nanoclusters: Application to the sensitive voltammetric determination of the cancer biomarker alpha fetoprotein

Wen Xiang[1] · Guanwu Wang[1] · Shuang Cao[1] · Qiuguo Wang[1] · Xiangyue Xiao[1] · Ting Li[1] · Minghui Yang[2]

Abstract

The authors describe a sensitive electrochemical immunoassay for the cancer biomarker α-fetoprotein (AFP). It is based on a combination of an immunoassay with DNA-based signal amplification. Two-dimensional MnO$_2$ nanosheets modified with gold nanoclusters (AuNC-MnO$_2$) were synthesized through one-pot process and utilized as an electrochemical probe. Bovine serum albumin served as templating agent to guide the formation and assembly of the modified sheets. The detection antibody against AFP and a polycytosine DNA sequence (dC$_{20}$) were immobilized onto the modified nanosheets. The electrochemical assay follows the usual sandwich protocol. The antibodies on the nanosheets then bind to AFP, while dC$_{20}$ causes signal amplification. The reaction of the phosphate backbone of dC$_{20}$ with molybdate leads to the formation of redox-active molybdophosphate which generates an electrochemical current, typically measured at 0.20 V (vs. Ag/AgCl). The method allows AFP to be determined in the 0.01 to 10 ng·mL^{-1} concentration range, and the detection limit is as low as 5 pg·mL^{-1}. This strategy overcomes the drawbacks of conventional immunoassays whose sensitivity is often limited because many immunoassays are rather difficult to amplify. The method has a wide scope in that various other DNA signal amplification methods such as rolling circle amplification and hybridization chain reactions may also be applied.

Keywords Alpha fetoprotein · Gold clusters · Biomimetic mineralization · Electrochemical · Molybdate · Molybdophosphate

Introduction

Aptamers are an alternative to traditional antibodies as binding molecules to different analyte targets, but immunoassays with antibody are still the dominated assay for commercial applications [1, 2]. However, the drawbacks of immunoassays are that their signal amplification strategies are rather limited, so the sensitivity is often not high enough for the detection of low level of analytes. On the contrary, DNA based signal strategies are versatile and signal amplification capability are strong. Previous efforts have explored trying to combine the specificity of an immunoassay with DNA based signal amplification strategies, such as immunoassays with PCR (immuno-PCR) and immunoassays with RCA (immuno-RCA) [3, 4]. However, these methods are still rather complexed and time consuming.

Protein based biomimetic mineralization method is the utilization of proteins as template for the synthesis of various nanomaterials under mild reaction conditions [5, 6]. Proteins that play the key role in biomimetic mineralization are with diverse functional groups like –COOH, –NH2, –SH, and will be driven to form versatile assembles according to the pH values [7]. This feature makes them excellent templates to guide the formation of diverse nanomaterials. Formerly, our group demonstrated the synthesis of biocompatible hematite (α-Fe$_2$O$_3$) and metal sulfide nanoparticles using bovine serum

✉ Ting Li
liting001@csu.edu.cn

✉ Minghui Yang
yangminghui@csu.edu.cn

[1] Department of General Surgery, The Second Xiang-ya Hospital, Central South University, Changsha 410011, China

[2] College of Chemistry and Chemical Engineering, Hunan Provincial Key Laboratory of Efficient and Clean Utilization of Manganese Resources, Central South University, Changsha, China

albumin (BSA) or even egg white as template [6]. In addition, BSA has also been proved capable of templating fluorescent metal clusters, such as gold nanocluster (AuNCs), silver nanocluster (Ag NCs), and copper nanocluster (Cu NCs) [8, 9].

In this work, we prepared electrochemical immunoassay for detection of cancer biomarker trying to combine antibody based immunoassay with DNA based signal amplification strategy. AuNCs anchored 2D MnO_2 nanosheets (AuNC-MnO_2) were synthesized by the above mentioned biomimetic mineralization guided method utilizing BSA as template. The nanosheets were utilized as supporting matrix for both detection antibody (Ab$_2$) and DNA strand due to the large specific surface area and good redox activity of MnO_2 nanosheets. The AuNCs on the MnO_2 nanosheets were utilized to adsorb antibody and conjugate polycytosine DNA sequence (dC$_{20}$). The electrochemical immunoassay was prepared by the traditional sandwich type protocol and alpha fetoprotein (AFP) was selected as a model protein biomarker to test the assay design methodology [10]. After capturing of the AuNC-MnO_2 nanosheets onto electrode based on the specific binding between antibody and antigen, the reaction of DNA strand on the nanosheet surface with molybdate formed redox molybdophosphate and generated electrochemical current [11–13]. The potential application of the immunoassay was demonstrated by analyzing AFP in human serum samples. This assay design method can find wide applications by further combing various DNA signal amplification technique.

Experimental section

Reagents and apparatus

Mouse monoclonal anti-AFP antibody and AFP antigen were purchased from Abcam (Cambridge, UK, http://www.abcam.cn/). Sodium molybdate dihydrate ($Na_2MoO_4.2H_2O$) was bought from Sigma-Aldrich (http://www.sigmaaldrich.com). Thiol group modified polycytosine (dC$_{20}$) was synthesized and purified by Sangon Biotech Co., Ltd. (Shanghai, China, http://www.sangon.com/). Other reagents were of analytical grade and used without further purification. All stock solutions were prepared with double-distilled water.

Electrochemical measurements were performed on a CHI-650D electrochemical workstation (Shanghai CH Instruments Co., China). A conventional three-electrode system was used with a glassy carbon electrode (GC, 3 mm in diameter) as the working electrode, an Ag/AgCl electrode as the reference electrode and a platinum wire as the auxiliary electrode. Transmission electron microscopy (TEM) was conducted on a Titan G2 60–300 transmission electron microscope (FEI, USA).

Synthesis of AuNC-MnO_2 nanosheets

AuNC-MnO_2 nanosheets were prepared through a one-pot procedure. Typically, 100 μL of BSA solution (250 mg mL^{-1}) was mixed with 450 μL of water. Then, 200 μL of Mn(NO$_3$)$_2$ solution (50 mM) and 200 μL of aqueous HAuCl$_4$ solution (25 mM) were added dropwise into the BSA solution. After that, 50 μL of NaOH solution (5 M) was added into the mixture. The final concentration of BSA, Mn^{2+}, $[AuCl_4]^-$ and OH^- were 25 mg mL^{-1}, 10 mM, 5 mM and 250 mM. The mixture was incubated at 37 °C for 12 h with vigorous stirring. After cooling to room temperature, the mixture was purified by dialysis (molecular weight cut-off MWCO = 14 kDa) against water for 24 h to remove excess salts and NaOH. The final solution was stored at 4 °C.

Preparation of the electrochemical immunoassay

Before construction of the electrochemical immunoassay, AuNC-MnO_2 nanosheet based electrochemical probe was first prepared. Into AuNC-MnO_2 solution (1 mM), detection AFP antibody (Ab$_2$) and dC$_{20}$ DNA strands were added to reach an antibody concentration of 10 μg.mL^{-1} and dC$_{20}$ concentration of 100 μM. The mixture solution was incubated for 8 h and then centrifuged to remove the free antibodies and DNA strands. The product was then dispersed into solution and stored before use.

For preparation of the immunoassay, capture AFP antibodies (Ab$_1$) were immobilized onto graphene oxide (GO) modified electrode surface. First, GO was dispersed into chitosan solution (0.5 mg.mL^{-1}, dissolved in water) to reach a concentration of 3 mg.mL^{-1}. Then, 5 μL of the composite solution was dropped onto electrode surface. After dried, the resulted electrode was incubated with glutaraldehyde (2.5%) solution for 30 min and then with Ab$_1$ solution (1 μg.mL^{-1}) for 1 h. After gentle wash, the electrode was immersed into BSA (1%) solution for 30 min to block nonspecific binding sites. Subsequently, the modified electrode was incubated with different concentrations of AFP standard solution for 1 h. With another round of wash, the electrode was incubated with the above synthesized AuNC-MnO_2 probe for 1 h.

For electrochemical testing, 5 μL of 6 mM Na_2MoO_4 solution was added onto the electrode surface and incubated for 20 min. Then, the electrode was tested in 0.5 M H_2SO_4. For cyclic voltammetry (CV) measurements, scan rate of 0.1 V/s was applied. For square wave voltammetry (SWV) testing, the amplitude applied was 0.025 V with frequency of 15 Hz. The SWV current at a peak potential of 0.18 V was recorded to draw the calibration plot.

Results and discussion

The AuNC-MnO$_2$ nanosheet was chosen as supporting matrix to prepare the electrochemical probe since the AuNC-MnO$_2$ nanosheet can be synthesized via one-pot procedure. The AuNCs was selected to be modified onto the nanosheet since AuNCs has good stability. The large surface area of the nanosheet can increase the loading of AuNCs, and then the loading of antibody as well as dC$_{20}$ DNA strand.

Scheme 1 shows the schematic representation for the synthesis of the AuNC-MnO$_2$ nanosheet based probe and the electrochemical immunoassay preparation as well as detection process. The novelty of this work is the combing of the antibody-antigen based immunoreaction with DNA based signal amplification strategy. The DNA based signal amplification is the reaction of DNA with molybdate to form redox molybdophosphate and generate electrochemical current [14–18]. The dC$_{20}$ DNA strand is chosen as our previous work has demonstrated the cytosine nucleobases can induce the highest electrochemical current intensity when reacted with molybdate [19].

The AuNC-MnO$_2$ nanosheet was synthesized based on biomimetic mineralization guided method with BSA acted as the template according to our previous work [20]. In that work, we utilized the AuNC-MnO$_2$ nanosheet as probe for fluorometric/magnetic bimodal sensing. To synthesize the AuNC-MnO$_2$ nanosheet, typically, Mn^{2+} and [AuCl$_4$]$^-$ were first mixed with BSA aqueous solution under vigorous vortexing. BSA plays the key role in biomimetic

mineralization process, which contains abundance of carboxyl groups and thiol groups. These functional groups can seize the Mn^{2+} and [AuCl$_4$]$^-$ to form BSA-Mn and BSA-Au complexes. Then, with the addition of NaOH into the above solution, the nucleation and growth of 2D MnO$_2$ and AuNCs were triggered. BSA acted here as both template and reductant in the whole synthesis process. On one hand, for MnO$_2$ nanosheets formation, the Mn ions that seized by BSA will initially turn into Mn(OH)$_2$ through hydrolysis reaction, and the intermediate Mn(OH)$_2$ will then be oxidized to MnO$_2$ with the help of dissolved oxygen. On the other hand, for AuNCs formation, reductive BSA molecules will reduce the [AuCl$_4$]$^-$ ions that entrapped by BSA to form AuNCs. Further interactions between BSA-MnO$_2$ nanosheets and BSA-AuNCs resulted in AuNC-MnO$_2$ assemblies with the help of BSA. BSA played another important role as "glue" in this progress.

The morphology and structure of the AuNC-MnO$_2$ were characterized by TEM. As shown in Fig. 1, TEM images show the AuNC-MnO$_2$ nanocomposite are flat 2D nanosheets with dimensions about 50–100 nm (Fig. 1a). The AuNC were observed successfully interspersed on the surface of 2D MnO$_2$ nanosheets with a mean size of around 2 nm (Fig. 1 b and c).

After the succseful synthesis of AuNC-MnO$_2$ nanosheets, to turn the nanosheets into electrochemical probe, Ab$_2$ and dC$_{20}$ DNA strands were both immobilized onto the nanosheets surface via AuNCs. Ab$_2$ were directly adsorbed onto AuNCs, while the dC$_{20}$ DNA strands were conjugated onto AuNCs through the thiol moiety at the end of the DNA strands. The electrochemical reaction of the functionalized

Scheme 1 Schematic representation for the synthesis of the AuNC-MnO$_2$ nanosheet based probe and the electrochemical preparation as well as detection process
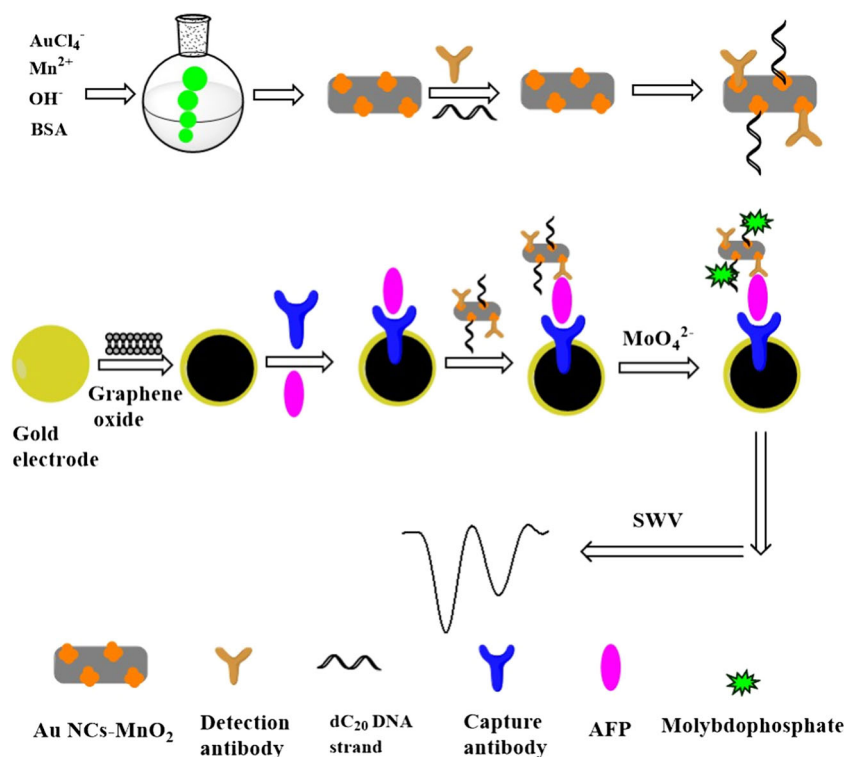
nanosheets with molybdate was then studied. Two electrodes were prepared, one with the immobilization of un-functionalized AuNC-MnO$_2$ nanosheets onto electrode, and one with the immobilization of functionalized AuNC-MnO$_2$
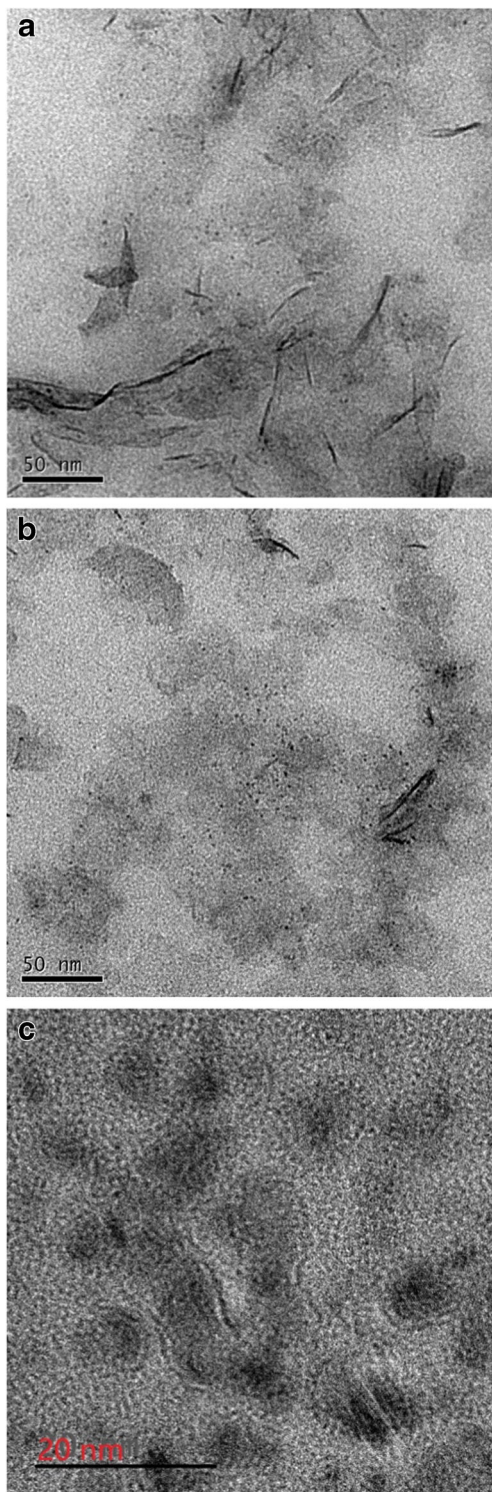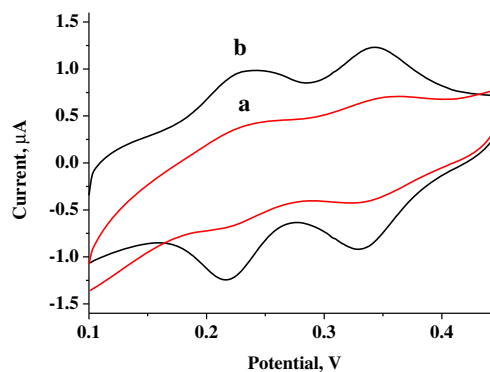

Fig. 2 Cyclic voltammetry responses of the electrodes immobilized with un-functionalized AuNC-MnO$_2$ nanosheets (a) and with Ab$_2$ as well as dC$_{20}$ DNA strands functionalized AuNC-MnO$_2$ nanosheets

nanosheets onto electrode. After the reaction of the two electrodes with molybdate, the electrodes were characterized in 0.5 M H$_2$SO$_4$ by cyclic voltammetry. For the electrode modified with un-functionalized AuNC-MnO$_2$ nanosheets, a pare of relatively small redox current is observed (Fig. 2, curve a). The generated electrochemical current can be ascribed to the reaction of molybdate itself on the electrode surface. On the contrary, for the functionalized AuNC-MnO$_2$ nanosheets
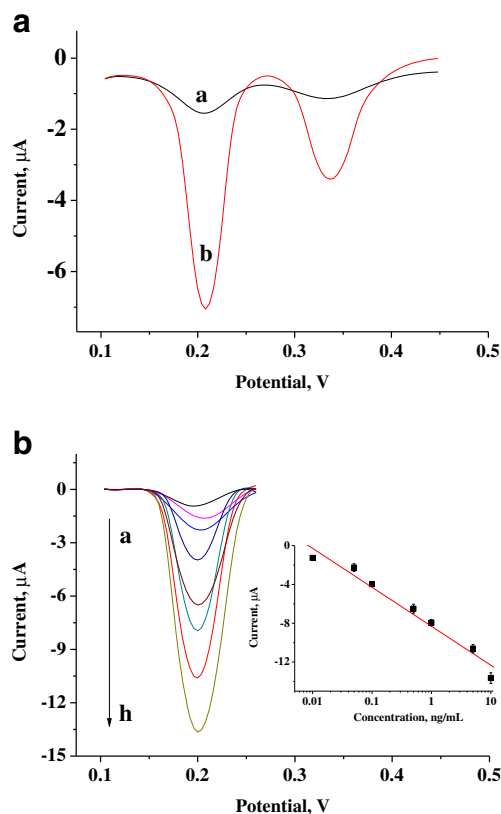

Fig. 3 a SWV responses of the immunoassay for blank samples (a) and for 1 ng.mL^{-1} of AFP (b). b Responses of the immunoassay to different concentrations of AFP, from a to h, 0, 0.01, 0.05, 0.1 0.5, 1, 5, 10 ng.mL^{-1}. The inset is the calibration plot. The current variations at 0.2 V were recorded to establish the calibration plot. Error bar = SD ($n = 3$)

Fig. 1 TEM images of the MnO$_2$ nanosheets (a) and AuNC-MnO$_2$ nanosheets ((b), low magnification; (c) high magnification)

Table 1　An overview of literature reports of electrochemical immuno for determination of AFP

Signal probe	Linear range	Detection limit	Reference
Cadmium alginate nanobeads	0.01 to 100 ng.mL^{-1}	10 pg.mL^{-1}	[21]
Thionin/reduced graphene oxide/gold nanoparticles	0.1–100.0 μg.mL^{-1}	50 ng.mL^{-1}	[22]
Au–Pd nanocrystals	0.05–30 ng.mL^{-1}	5 pg.mL^{-1}	[23]
Azure A	0.01 to 25 ng.mL^{-1}	3.3 pg.mL^{-1}	[24]
dC$_{20}$ DNA strand	0.01 ng.mL^{-1} to 10 ng.mL^{-1}	5 pg.mL^{-1}	This work

modified electrode, a pare of rather strong current peaks is observed at around of 0.22 and 0. 37 V (Fig. 2, curve b). The strong electrochemical current generated is due to the reaction of dC$_{20}$ DNA on the nanosheets with molybdate, specifically, the reaction phosphate backbone of dC$_{20}$ DNA with molybdate that formed molybdophosphate. The electron transfer within the formed redox molybdophosphate lead to the two pairs of redox peaks. These data proved the possibility of the functionalized AuNC-MnO$_2$ nanosheets as electrochemical probe.

Then, AFP, as a model analyte target was chosen to test the immunoassay design methodology utilizing the AuNC-MnO$_2$ nanosheet as electrochemical probe. The immunoassay was prepared based on sandwich structure. Graphene oxide (GO) was used as supporting matrix for Ab$_1$. After the following capturing of AFP and the functionalized AuNC-MnO$_2$ nanosheets onto electrode through immuno-reaction, the nanosheet can generate electrochemical current. Initially, to demonstrate the possibility of the for AFP detection, two immunoelectrodes were prepared, one for the detection of blank sample and one for the detection of 1 ng.mL^{-1} of AFP. The two immunos were characterized in 0.5 H$_2$SO$_4$ by square wave voltammetry (SWV). From Fig. 3a, we can see that of the immunoelectrode prepared for blank sample, only small background current peaks are observed. However, of the immunoelectrode for the detection of 1 ng.mL^{-1} of AFP, the electrode generates strong current peaks. These results proved

the possibility of the immunoassay to discriminate samples with and without target AFP.

To determine the linear range of the immuno towards AFP, a series of immunoelectrodes were prepared for the detection of different concentrations of AFP. Figure 3b shows the responses of the immunoelectrodes. It can be seen the peak current at 0.2 V is increased with the increase of AFP concentrations. A linear range between current response and logarithm of HER2 concentration in the range from 0.01 ng.mL^{-1} to 10 ng.mL^{-1} is obtained (inset of Fig. 3b) with limit of detection calculated to be 5 pg.mL^{-1} (based on S/N of 3).

The analytical performance of the immunoassay is compared with previous reported electrochemical immunoassays for AFP detection. From Table 1, it can be seen that the performance of the immunoassay is comparable or even better than literature reports.

Besides the linear range and limit of detection, good selectivity of the immunoassay is also of great importance for precise detection of analyte target in real serum samples. To test the selectivity of the immunoassay, several potential interferences that may coexist with AFP in human serum samples, including human IgG, human epidermal growth factor receptor 2 (HER2), p53, carcinoembryonic antigen (CEA) and CA125 were studied. As shown in Fig. 4, the responses of the immunoassay to 10 ng.mL^{-1} of the above interference are close to response of the immunoassay to blank sample, demonstrating good selectivity.
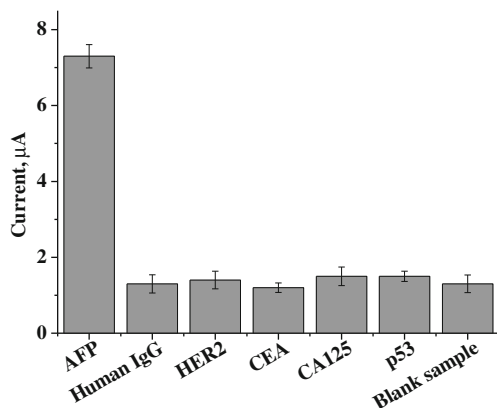
Fig. 4 Responses of the immunoassay to different proteins and blank sample
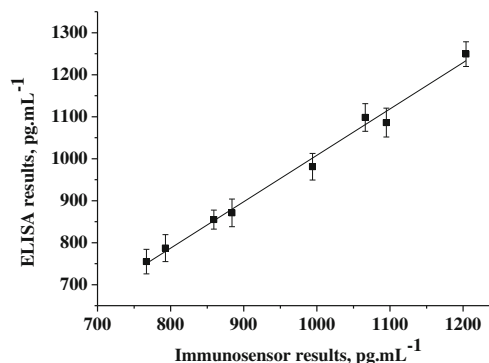
Fig. 5 Compare the AFP level in serum samples determined by the immuno with those determined by ELISA kit. Error bar = SD ($n = 3$)

The precision of the immunoassay were evaluated by testing each concentration of AFP five times independently. Experimental data indicates that for testing 0.1 and 1 ng. mL^{-1} of HER2, the relative standard deviation of the immunoassay results are 1.1 and 1.6%, respectively, indicating the immunoassay results are reliable.

Finally, to demonstrate potential clinical application of the immunoassay, AFP levels in human serum samples were tested. Serum samples were initially diluted by phosphate buffer to minimize matrix effect and then measured by the assay. The samples were also tested by commercial ELISA kit and the two results were compared. As shown in Fig. 5, AFP levels in the samples analyzed by the two methods agreed well, and a straight plot is obtained with a correlation coefficient of 0.993. This demonstrates that the testing results of the immunoassay are similar to that of the commercial ELISA kit, further supporting potential application of the immunoassay in clinical areas.

Conclusions

In summary, we reported electrochemical immunoassay for cancer biomarker detection through combing the antibody-antigen immunoreaction with DNA based signal generation strategy. This method paves new way for electrochemical immunoassays by integrating the high specificity of antibody based immunoassay and the versatility as well as high signal amplification capability of DNA based signal amplification strategy. The immunoassay can be applied to the detection of other analytes using different antibodies. The sensitivity of the assay can be further improved, for example, various DNA based signal amplification strategies, such as rolling circle amplification (RCA) and hybridization chain reaction (HCR) can be applied to the immunoassay design to further enhance the sensitivity of the immunoassay.

References

1. Cheng X, Cen Y, Xu G, Wei F, Shi M, Xu X, Sohail M, Hu Q (2018) Aptamer based fluorometric determination of ATP by exploiting the FRET between carbon dots and graphene oxide. Microchim Acta 185(2):144

2. Song Y, Xu G, Wei F, Cen Y, Sohail M, Shi M, Xu X, Ma Y, Ma Y, Hu Q (2018) Aptamer-based fluorescent platform for ultrasensitive adenosine detection utilizing Fe3O4 magnetic nanoparticles and silver nanoparticles. Microchim Acta 185(2):139

3. Zhang X, Zhuang H (2018) A carbon nanotube-enhanced real-time immuno-PCR for ultrasensitive detection of AHTN in water. Anal Biochem 544:22–28

4. Ebai T, Souza de Oliveira FM, Lof L, Wik L, Schweiger C, Larsson A, Keilholtz U, Haybaeck J, Landegren U, Kamali-Moghaddam M (2017) Analytically sensitive protein detection in microtiter plates by proximity ligation with rolling circle amplification. Clin Chem 63(9):1497–1505

5. Wang L, Li X, Jiang X, Chen W, Hu L, Walle MD, Deng L, Yang M, Liu YN, Kirin SI (2015) When protein-based biomineralization meets hydrothermal synthesis: the nanostructures of the as-prepared materials are independent of the protein types. Chem Commun 51 (96):17076–17079

6. Fei X, Li W, Shao Z, Seeger S, Zhao D, Chen X (2014) Protein biomineralized nanoporous inorganic mesocrystals with tunable hierarchical nanostructures. J Am Chem Soc 136(44):15781–15786

7. Sheng J, Wang L, Han Y, Chen W, Liu H, Zhang M, Deng L, Liu Y-N (2018) Dual Roles of Protein as a Template and a Sulfur Provider: A General Approach to Metal Sulfides for Efficient Photothermal Therapy of Cancer. Small 14(1):1702529

8. Lu Y, Chen W (2012) Sub-nanometre sized metal clusters: from synthetic challenges to the unique property discoveries. Chem Soc Rev 41(9):3594–3623

9. Diez I, Ras RH (2011) Fluorescent silver nanoclusters. Nanoscale 3 (5):1963–1970

10. Zhang P, Huang H, Wang N, Li H, Shen D, Ma H (2017) Duplex voltammetric immunoassay for the cancer biomarkers carcinoembryonic antigen and alpha-fetoprotein by using metal-organic framework probes and a glassy carbon electrode modified with thiolated polyaniline nanofibers. Microchim Acta 184(10): 4037–4045

11. Huang Y, Tang C, Liu J, Cheng J, Si Z, Li T, Yang M (2017) Signal amplification strategy for electrochemical immunosensing based on a molybdophosphate induced enhanced redox current on the surface of hydroxyapatite nanoparticles. Microchim Acta 184(3):855–861

12. Xie B, Zhou N, Ding R, Zhao Y, Zhang B, Li T, Yang M (2017) Dual signal amplification strategy for electrochemical detection of platelet-derived growth factor BB. Anal Methods 9(46):6569–6573

13. Shen C, Li X, Rasooly A, Guo L, Zhang K, Yang M (2016) A single electrochemical biosensor for detecting the activity and inhibition of both protein kinase and alkaline phosphatase based on phosphate ions induced deposition of redox precipitates. Biosens Bioelectron 85:220–225

14. Jiang W, Liu L, Zhang L, Guo Q, Cui Y, Yang M (2017) Sensitive immunosensing of the carcinoembryonic antigen utilizing aptamer-based in-situ formation of a redox-active heteropolyacid and rolling circle amplification. Microchim Acta 184(12):4757–4763

15. Jiang W, Tian D, Zhang L, Guo Q, Cui Y, Yang M (2017) Dual signal amplification strategy for amperometric aptasensing using hydroxyapatite nanoparticles. Application to the sensitive detection of the cancer biomarker platelet-derived growth factor BB. Microchim Acta 184(11):4375–4381

16. Shen C, Zeng K, Luo J, Li X, Yang M, Rasooly A (2017) Self-assembled DNA generated electric current biosensor for HER2 analysis. Anal Chem 89(19):10264–10269

17. Feng K, Liu J, Deng L, Yu H, Yang M (2018) Amperometric detection of microRNA based on DNA-controlled current of a molybdophosphate redox probe and amplification via hybridization chain reaction. Microchim Acta 185(1):28

18. Li X, Shen C, Yang M, Rasooly A (2018) Polycytosine DNA electric-current-generated Immunosensor for electrochemical

detection of human epidermal growth factor Receptor2 (HER2). Anal Chem 90(7):4764–4769

19. Hu L, Hu S, Guo L, Shen C, Yang M, Rasooly A (2017) DNA generated electric current biosensor. Anal Chem 89(4):2547–2552

20. Sheng J, Jiang X, Wang L, Yang M, Liu Y-N (2018) Biomimetic mineralization guided one-pot preparation of gold clusters anchored two-dimensional MnO2 Nanosheets for Fluorometric/magnetic bi-modal sensing. Anal Chem 90(4):2926–2932

21. Wang Z, Liu N, Feng F, Ma Z (2015) Synthesis of cadmium, lead and copper alginate nanobeads as immunosensing probes for the detection of AFP, CEA and PSA. Biosens Bioelectron 70:98–105

22. Li G, Li S, Wang Z, Xue Y, Dong C, Zeng J, Huang Y, Liang J, Zhou Z (2018) Label-free electrochemical aptasensor for detection of alpha-fetoprotein based on AFP-aptamer and thionin/reduced graphene oxide/gold nanoparticles. Anal Biochem 547:37–44

23. Zhao L, Li S, He J, Tian G, Wei Q, Li H (2013) Enzyme-free electrochemical immunosensor configured with au-Pd nanocrystals and N-doped graphene sheets for sensitive detection of AFP. Biosens Bioelectron 49:222–225

24. Zhao J, Guo Z, Feng D, Guo J, Wang J, Zhang Y (2015) Simultaneous electrochemical immunosensing of alpha-fetoprotein and prostate specific antigen using a glassy carbon electrode modified with gold nanoparticle-coated silica nanospheres and decorated with azure a or ferrocenecarboxylic acid. Microchim Acta 182(15–16):2435–2442